

2023

Relating Quantitative Ultrasound Measurements of Two Cancer Cell Lines, HeLa and MDA-MB-231, to Biological Markers

Ashleigh Hughes

Follow this and additional works at: <https://digitalcommons.assumption.edu/honorstheses>



Part of the [Life Sciences Commons](#)

Relating Quantitative Ultrasound Measurements of Two Cancer Cell Lines, HeLa and
MDA-MB-231, to Biological Markers

Ashleigh Hughes

Faculty Supervisor: Maria-Teresa Herd, Ph.D.

Department of Biological and Physical Sciences

A Thesis Submitted to Fulfill the Requirements of the Honors Program at Assumption University

Fall 2022

Ashleigh Hughes

6 December 2022

Abstract

Quantitative ultrasound is a promising alternative method for cancer diagnosis that is non-invasive and cost-effective. This experiment investigated the potential of quantitative ultrasound in diagnosing and differentiating breast and cervical cancer. Using HeLa cells and MDA cells, the speed of sound and attenuation was measured using 5, 10, and 15 MHz transducers. It was found that the speed of sound of the MDA and HeLa cells did not deviate much, with values of 1527.6 ± 3.1 m/s and 1527.5 ± 3.9 m/s, respectively, but the attenuation of the MDA and HeLa did vary, though error in the experiment leaves this conclusion up for debate. Lack of variation in the speed of sound could have been due to the similar densities of the cell pellets as well as similar cancerous morphologies of the cells. The difference in attenuation was likely due to increased interference from the MDA cells due to unique mutations. Overall, additional experiments need to be done to finalize the attenuation conclusions. In addition, it must be explored if other ultrasonic characteristics can be used to differentiate between the cells and other cell lines or cancer types must be used to further investigate the potential of quantitative ultrasound.

Introduction

Quantitative Ultrasound

Cancer is the second most common cause of death in the United States; 1.9 million new cases are expected to be diagnosed in 2022 (1). Approximately 39.5% of the population will be diagnosed with cancer at some point in their lifetime, and the CDC predicts that by 2050, due to the growth and aging of the US population, cancer diagnosis will increase by 49% (2, 3).

Consequently, the cost of treatment is likely to increase (2). Due to the increased incidence and cost of cancer, it is crucial to streamline cancer diagnosis.

The most common existing methods used to diagnose cancer include lab tests, imaging tests, and surgical biopsies. Lab tests can help a health care team make a diagnosis by looking at chemicals or circulating tumor cells in the blood, but they do not provide a definitive diagnosis method and further testing is required (4). Imaging tests are used to look inside the body for various reasons; for example, searching for a tumor or diagnosing the stage of cancer, etc. However, like lab tests, these imaging results cannot confirm if an abnormal area is cancer. They can find large masses of cells, but not small ones, and can incorrectly indicate cancer (5). Therefore, to definitively diagnose cancer, biopsies are required. They are invasive and involve removing a tissue sample from the patient with either a needle or an endoscope (6). There are various types of biopsies; a needle biopsy involves using a needle to collect cells, an excisional biopsy involves surgery to remove suspect tissue, a shave biopsy removes tissue by scraping the surface of the skin, and endoscopic and laparoscopic biopsies insert tubes with video cameras to examine abnormal areas and take tissue samples for examination (7). Biopsies are the most invasive and expensive part of cancer diagnosis. Because of the extensive testing required, it is financially and medically beneficial to develop a less-invasive and less-expensive way to diagnose cancer and ultimately reduce the number of biopsies.

Ultrasound is a potential alternative method that is already used in medical imaging; for example, it is used for sonograms and diagnosing gallbladder disease. It is an inexpensive, versatile, and portable technique that may be preferable to existing methods for cancer diagnosis because of its low cost, non-invasive, non-radiation nature (8). Ultrasounds function by using sound waves to produce images from the inside of a patient's body (9); these images are created

by impedance mismatches or specular reflections caused by different types of tissues having different resistances to sound wave propagation. The mismatch between these resistances creates an image, and diffuse reflections where sound waves scatter off of tissues show gray-scale differences (Figure 1). The most well-established ultrasound method is B-mode imaging. This technique displays the brightness of the radio-frequency (RF) echo signal; these echoes are created by the scattering of ultrasonic waves in various directions by the various tissue types. Therefore, B-mode imaging can be used to qualitatively distinguish tissue types as each has a unique reaction to ultrasound waves (10). B-mode ultrasound imaging has been utilized in oncology to obtain data on tumors in an attempt to diagnose cancer. However, this is insufficient to definitively diagnose cancer and other methods are required.

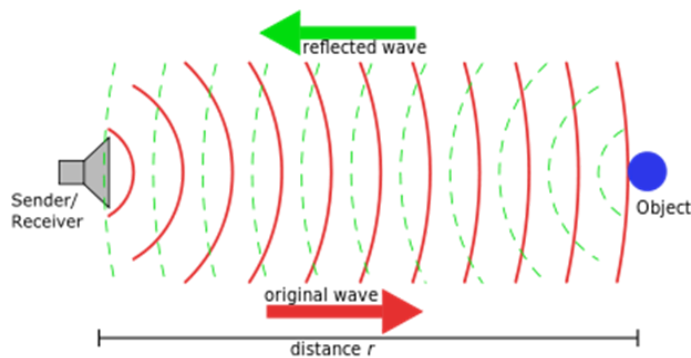


Figure 1: An image depicting the basic method by which ultrasounds create images. The sender/receiver sends original waves, as seen by the red waves. These waves then come in contact with the object which in this project is the tissue. The object then reflects the waves back, demonstrated by the green waves. The waves are reflected back at a different frequency due to impedance mismatches.

Quantitative ultrasound (QUS) utilizes the characteristics of tissues to quantitatively distinguish between tissue types. It differs from B-mode ultrasound because QUS provides quantitative information as opposed to visual, qualitative information. While B-mode ultrasound is used to form an image, QUS is used to obtain numerical values for specific measurements regarding the various characteristics of tissues. Obtaining QUS data requires collecting and processing the radio frequency (RF) data and ensuring the tissue properties are independent of instrumentation and operator. Further, these data need to be consistent and set throughout the industry. Some features of tissue types that can be examined by QUS are the speed of sound and attenuation. The speed of sound relates to the propagation of sound waves through tissues and tends to be higher in tissues with increased stiffness and density (11). Attenuation is the decay rate of a wave as it moves through a material. The intensity of ultrasound waves decreases as it travels through tissues because the tissue absorbs and scatters the waves (12). Finally, backscatter refers to the frequency-dependent reflection of waves back in the direction that they came (13). QUS properties are intrinsic to the tissue and do not depend upon instrumentation.

The QUS approach has been utilized in previous studies: one performed by Teisseire et al. (14) examined the ultrasonic backscatter coefficient of Chinese hamster ovary cells. This study used a hamster ovary cell pellet—a large cluster of collected cells—and compared its backscatter results against pre-existing models of backscatter. The researchers found that their experimental data agreed with pre-existing data, implying that the models are valid tools for classifying cell structures. Another study, performed by Doyle et al. (15), examined normal and cancerous breast cancer cells and how their ultrasonic qualities differed. The researchers sought to determine if cancerous breast cancer cells could be detected with high-frequency ultrasound. High-frequency ultrasound is ultrasound of at least 10 MHz which is used to visualize skin and

upper part of subcutaneous tissue. In this study, they used cell cultures treated with transducers to collect their data. They found that normal and malignant cells have qualities that are significantly different. Both of these studies examine how QUS can be used to diagnose cancer. This study had a similar goal; using QUS data, it examined the characteristics of two types of cancer to differentiate between them. Using these properties and QUS methods, cancer diagnosis can become non-invasive and cost-effective.

Cancer Types

Breast and cervical cancer are cancers that affect people worldwide. Breast cancer accounts for 22-25% of new cancer cases diagnosed (16, 17). Cervical cancer was the fourth most common cancer in women and accounted for 6.9% of all cancer cases diagnosed in 2020 (16). While lung cancer was the leading cause of cancer-related death, breast cancer accounted for 6.9% of cancer deaths. Female death rates for breast and cervical cancers were significantly higher in low and middle-income countries when compared to high-income countries (18). The American Cancer Society predicts that breast cancer will account for 31% of the new cancer cases diagnosed in 2022, with approximately 287,850 new cases (1). Cervical cancer is estimated to account for 14,000 new cases and 4,280 deaths in the United States (19). Due to the incidence and aggressiveness of these cancers, both nationally and worldwide, determining a fast and effective alternative diagnosis method for them is crucial.

Breast cancer is characterized by uncontrolled, abnormal growth of breast cells (20). Mutations in the genes *BRCA1*, *BRCA2*, *P53*, *PTEN*, and *ATM* can predispose people to breast cancer. Breast cancer has three major subtypes, and each is based on the presence or absence of estrogen (ER) and/or progesterone (PR) receptors and human epidermal growth factor 2 (HER2). Triple-negative breast cancer, where all three markers are absent (ER-negative, PR-negative,

HER2 not expressed), is extremely aggressive and lacks targeted therapies. Patients with triple-negative breast cancer typically have a poor prognosis; while the tumors are responsive to chemotherapy, they are more likely to recur than the other two subtypes (21, 22, 23, 24). As more than 90% of breast cancers are not metastatic at the time of diagnosis, it is crucial that breast cancer (especially triple-negative) be detected early (25). Triple-negative breast cancers grow quicker than other breast cancers, and they are more likely to be metastatic by the time it is discovered, and therefore the prognosis is not as positive. The 5-year survival rate for triple-negative breast cancer that has metastasized at the time of diagnosis is 12% (26). Breast cancer is typically initially diagnosed using a mammogram, a low-dose x-ray that detects abnormal areas in the breast. The goal of mammography is early cancer detection. However, mammograms cannot specifically determine if these abnormal areas are cancer, so further testing in the form of biopsies is typically required (25). Mammograms and biopsies are both painful methods of breast cancer detection. In addition, mammograms are a type of radiation exposure. Even in low doses, this can raise the risk of developing cancer, which does not make it an ideal method of diagnosis. Therefore, determining an alternative method of diagnosis would be safer and less painful for patients.

Cervical cancer is the fourth most common cancer in women worldwide (16). Cervical cancer occurs when the cells of the cervix - the lower part of the uterus that connects to the vagina - are genetically altered (27). Cervical cancer is almost always caused by chronic infection by high-risk subtypes of the human papillomavirus (HPV); specifically, HPV accounts for approximately 90% of all cervical cancer cases (28). However, HPV infection alone is not sufficient to cause cervical cancer; several environmental factors, such as smoking, and genetic factors, like mutations in the genes *TP53*, *MDM2*, and *CDKN2A*, are often involved in the

progression of a precancerous lesion to invasive cancer (29). Incidence and mortality of cervical cancer vary widely due to geographic location. In high-income countries, due to increased screening in the form of the Pap smear and the implementation of the HPV vaccine, cervical cancer incidence has decreased by more than half in the past 30 years. However, in low and middle-income countries, due to a lack of medical resources and infrastructure, cervical cancer remains the second most common type of cancer and the third most common cause of cancer-related death. Cervical cancer diagnosis is done in multiple steps; the woman typically receives a pelvic exam to visualize the cervix and vagina (27). Cervical cytology is also done; a sample of cells is taken from the cervix to check for any abnormalities (30). In symptomatic patients, a colposcopy and biopsy are performed to definitively diagnose cervical cancer (27). All of the methods for diagnosing cervical cancer are invasive and uncomfortable. As with breast cancer, determining an alternative, less-invasive method of diagnosis would increase patient comfort and the probability of patient compliance with testing guidelines.

Literature Review

Cancer

All cancers are characterized by abnormal and uncontrolled growth of mutated cells. These cells have the ability to leave their original site of growth, invade normal tissue, and metastasize to other areas of the body. Cells acquire this ability because the mutations cause the cells to stop their normal function and transform into cancerous cells (33). These mutations occur in proto-oncogenes. Proto-oncogenes are a class of genes that, when mutated, become oncogenes. Proto-oncogenes are typically genes that control cell growth development; they control cell division and regulate apoptosis, which is programmed cell death. These processes are crucial for healthy growth and development. However, when proto-oncogenes are mutated into

oncogenes, these functions are inhibited (34). These mutations can also occur in tumor suppressor genes (TSG). TSGs are involved in DNA damage repair, inhibition of cell division, induction of apoptosis, and suppression of metastasis (35). When these genes are mutated, cells divide uncontrollably, avoid apoptosis, and metastasize. These mutations are all required to stimulate cancerous growth and are characteristic of all types of cancer. The mutations can be caused by a variety of environmental and genetic factors and occur in any tissue in the body.

Cervical Cancer

As stated previously, cervical cancer is cancer of the cervix, the lower part of the uterus that connects to the vagina (35). About 80% of cervical cancer cases arise from dysplasia, or abnormally developed cells, in the squamous tissue of the cervix. Squamous cell carcinoma, which is cancer in the epithelial lining of the outer part of the cervix projecting into the vagina, accounts for 80% of all cervical cancer cases. Adenocarcinoma of the cervix, which is cancer of the glandular cells lining the cervical canal, accounts for 20% of the cases (36, 37). Cervical cells are typically mutated due to infection by high-risk subtypes of the human papillomavirus (HPV) (38).

HPV is considered a casual agent in cervical cancer. HPV is classified as high risk (HR-HPV) and low risk (LR-HPV) according to its carcinogenic potential (39). There are fourteen HR-HPV subtypes; HPV16 and HPV18 are responsible for most cervical cancers (40). HR-HPV is typically associated with invasive cervical cancer; persistent or repeated infection is characteristic of cervical carcinogenesis. HPV infects epithelial cells of the cervix via lesions. Infected cells then develop high-grade lesions which can lead to cervical neoplasia (abnormal growth of tissue) and eventually invasive cancer. When the virus is integrated into the host cell's genome, the virus can mutate cells to favor virus replication and cell transformation (39).

HPV is a circular DNA virus with eight genes. These genes are characterized as early or late according to their expression in the progression of HPV; there are six early genes, called *E1*, *E2*, *E3*, *E4*, *E5*, and *E6*, and two late genes, called *L1* and *L2*. Integration of HPV into the genome typically occurs because of a break in the *E2* gene. *E6* and *E7* are the genes primarily responsible for cancerous transformation; they are the oncogenes of HPV. They directly influence cellular pathways like apoptosis, cell proliferation, growth, and motility. *E2* is the main repressor of the expression of *E6* and *E7*. Breaking the *E2* genes leads to the loss of repression of the oncogenes. Activation of *E6* and *E7* leads to the onset of tumorigenesis (39).

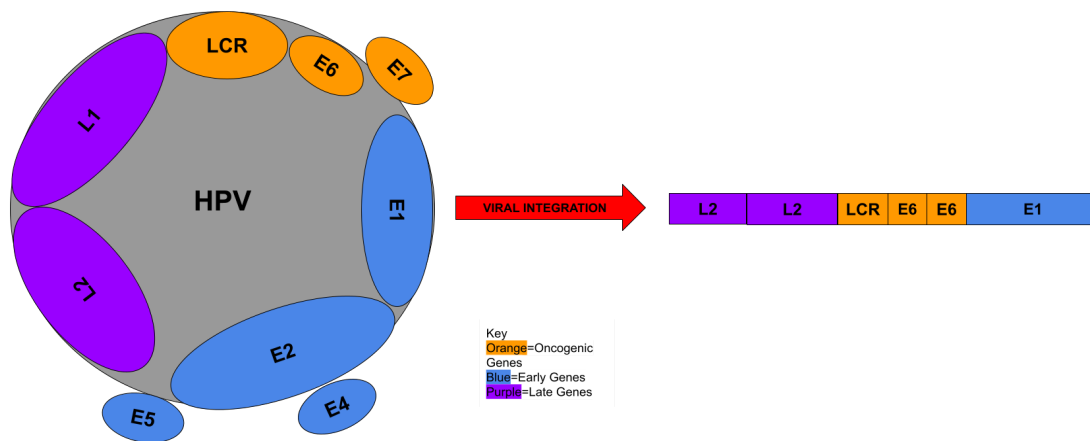


Figure 2: An image depicting the structure of the HPV gene. HPV is a circular virus with eight genes and one long control region (LCR) with areas for transcriptional activators and repressors. Genes are color-coded based on their expression time (early or late) and their oncogenic potential. Integration into the genome can result in the loss of the *E2* gene and activation of oncogenes.

Specifically, oncogene *E6* makes products that inhibit *p53* and *Bak* (39). *p53* is a tumor suppressor gene that controls cell division and cell death (41). *Bak* is a member of the *BCL2* protein family and acts as a regulator of apoptosis (42). *E6* also promotes cell proliferation by upregulating telomerase activity, which leads to cellular immortalization. *E6* affects *paxillin*, which binds to proteins involved in actin cytoskeleton organization (39). Actin plays a role in cell motility and is directly associated with tumor metastasis (43). *E6*'s control of *paxillin* leads to the rupture of the cytoskeleton, which allows cancerous cells to invade the extracellular matrix and metastasize to other tissues of the body. *E6* also affects *IRF-3*, which decreases transcription of the *INF-b* gene, leading to increased cellular proliferation. Finally, *E6* targets *Bax* and *C-myc*, which leads to an anti-apoptotic effect (39).

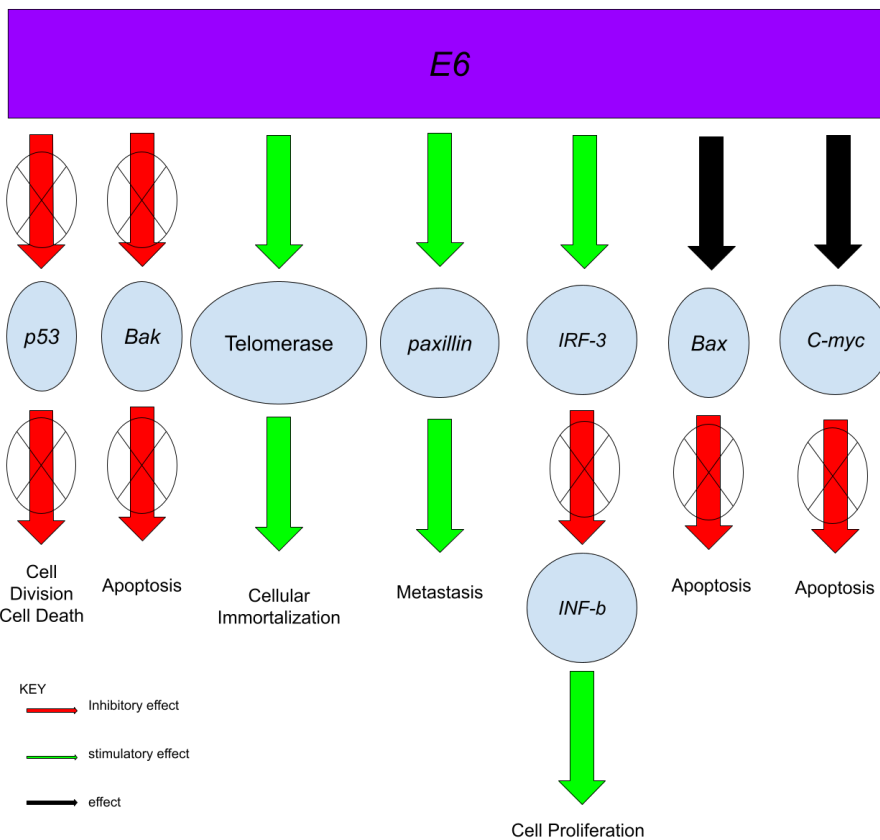


Figure 3: An image depicting the genes that are impacted by the *E6* oncogene. The activation or suppression of the various genes leads to a carcinogenic effect on cells, such as suspension of apoptosis and cell division control or increased cell proliferation, metastasis, and cellular immortalization.

Similarly, *E7* inhibits *pRB*, which leads to *p16* upregulation and *CDK-1* inactivation. *p16* and *CKD-1* are tumor suppressor genes; *E7*'s alteration of the genes leads to tumor proliferation. *E7* also stimulates the production of cyclins A and E, inactivates *p21* and *p27*, and amplifies centrioles. All of these mechanisms lead to cell immortalization (39). By altering the above genes, overexpression of *E6* and *E7* can initiate the cellular transformation process.

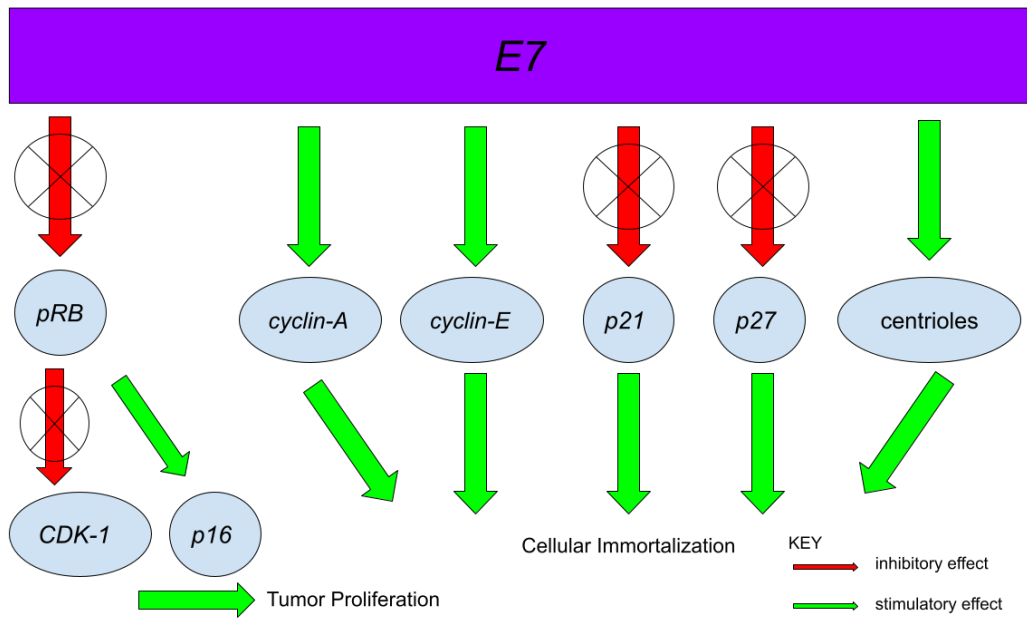


Figure 4: An image depicting the genes that are impacted by the *E7* oncogene. *E7* can negatively inhibit or stimulate genes and lead to both tumor proliferation and cellular immortalization.

While HPV infections are necessary to develop cervical cancer, they are not sufficient; only 99% of cervical cancers are caused by cervical cancer, and it is widely reported that some women develop cervical cancer independently of HPV infection. The success of the HPV

infection in causing cervical cancer depends on interactions between the host cell and the viral genome. There is evidence that host genetics play a role in cervical cancer susceptibilities, such as familial aggregation of cervical neoplasia in cervical cancer first-degree relatives, twin studies, and Fanconi anemia patients. However, the specific genes which increase a patient's susceptibility to cervical cancer are unknown. Several studies have been conducted looking at tumor suppressor genes such as *TP53*, *MDM2*, *CDKN2A*, and *CDKN1A*, but no definitive evidence has shown that mutations in these genes increase susceptibility to cervical cancer (44).

Of specific relevance to this study is the HeLa cervical cancer cell line. The HeLa cell line was isolated from a cervical adenocarcinoma in a 31-year-old African-American woman in 1951 (32). As is the case with most cervical cancers, the cells have HPV DNA, indicating that this illness was caused by HPV (45). 4.5 million single-nucleotide variations (SNVs) have been found in the HeLa cell lines. About 3,000 structural variations have also been identified, including deletions, insertions, and translocations. These mutations caused 2,000 genes to be overexpressed, resulting in increased proliferation and transcription (46). HeLa cells also display chromothripsis, or chromosome shattering. Chromothripsis is when tens of thousands of chromosomal arrangements occur. This can lead to oncogene activation and tumor suppressor loss (47). However, it is unknown if the set of rearrangements caused carcinogenesis or if these rearrangements occurred during cell culture. (46).

Of the mutations that occur in HeLa, there were 10 preferentially essential genes that have the lowest mean subtracted score of the cell line. These genes were the most essential in causing carcinogenic growth (48). The first was the *UBE3A* gene, which provides instructions for making ubiquitin protein ligase E3A, which helps regulate protein synthesis and degradation (19). This particular protein interacts with the *E6* protein of HPV-16 and HPV-18 and causes the

ubiquitination and proteolysis of p53, resulting in a loss of the tumor-suppressor gene (50). The *CRNKL1* gene is also mutated and is involved in pre-mRNA splicing and cell cycle progression (51, 52). Mutations result in a loss of cell cycle regulation (52). Next is the *URII* gene. This gene plays roles in ubiquitination and transcription and has been known to play roles in multiple malignancies (53). The *NOL7* gene controls cell growth rates and functions as a tumor suppressor. When mutated, the cell grows uncontrollably (54). The *ABCD1* gene provides instructions for producing the *ALDP* protein, which breaks down fatty acids (55). The *RNPI* gene encodes an integral membrane protein that forms part of the regulatory subunit of proteasome and thus mediates ubiquitination (56). The *ZERI* protein encodes a subunit of the *E3* ubiquitin ligase complex and may be involved in meiosis. Mutations can cause both errors in protein degradation and chromosome segregation before the division of gametes (57). The *GNRHI* protein encodes a preprotein that is processed to generate a peptide which is a member of the GnRH family of peptides (58). This family of proteins has been shown to play a role in regulating cell proliferation (59). The next protein, the *DCTN6* protein, encodes a protein called dynactin-1, which plays a critical role in cell division and cell transport (60). Finally, the *TNS2* belongs to the tensin family, which plays a role in regulating cell migration. Mutations can result in cell invasion and metastasis (61). A tabulated summary of these genes and their functions is listed below. All of these mutations and more play a role in the cancerous nature of HeLa cells and contributed to the transformation of the cervical cells.

Table 1: A list of the major genes mutated in HeLa cells, their function, and how a mutation in that gene can lead to cancerous growth.

Gene	Function	Mutation
<i>UBE3A</i>	Makes ubiquitin protein ligase E3A, which regulates protein synthesis and degradation	Interacts with the E6 protein of HPV-16 and HPV-18, and causes the ubiquitination and proteolysis of p53, resulting

		in a loss of the tumor-suppressor gene
<i>CRNKL1</i>	Pre-mRNA splicing, cell cycle progression	Loss of cell cycle regulation
<i>URI</i>	Ubiquitination, transcription	Specific method is unknown; known to play role in multiple malignancies
<i>NOL7</i>	Controls cell growth rates, tumor suppressor	Hyperplasia
<i>ABCD1</i>	Instructions for producing <i>ALDP</i> protein, which breaks down fatty acids	Unknown
<i>RNP1</i>	Encodes integral membrane protein forming regulatory subunit of proteasome, regulates ubiquitination	Dysregulation of ubiquitination
<i>ZER1</i>	Encodes subunit of <i>E3</i> ubiquitin ligase, involved in meiosis	Errors in protein degradation and chromosome segregation before the division of gametes
<i>GNRH1</i>	Encodes preprotein processed to generate peptide which is a member of <i>GnRH</i> family	Dysregulation of cell proliferation; hyperplasia
<i>DCTN6</i>	Encodes dynactin-1, which controls cell division and transport	Hyperplasia
<i>TNS2</i>	In the tensin family, which plays a role in regulated cell migration	Cell invasion and metastasis

Breast Cancer

Breast cancer is the uncontrolled, abnormal growth of breast cells and is the second most common cancer diagnosed in women, behind skin cancer (20). Unlike cervical cancer, there is not one overwhelming cause of breast cancer. However, there are multiple risk factors that

predispose one to breast cancer. Some are related to the level of hormones like estrogen and progesterone and how they fluctuate throughout a female's lifetime. The first relates to childbearing; generally, the risk of breast cancer is reduced by bearing children, which accounts for high rates of breast cancer in nuns and single women and low rates in married women (72). Women who had had at least one full-term pregnancy have about a 25% reduction in breast cancer risk. The younger one is at the age of their first birth, the greater their reduction in risk is. (72). Also, breastfeeding tends to have a protective effect, as breast cancer risk is low in areas where prolonged breastfeeding is common (72). However, the effect of breastfeeding is controversial as the decrease in risk associated with breast cancer is minimal. (73). Women who experience menopause late in life are more likely to develop breast cancer; the risk increases by 3% each year older at menopause (72). The use of oral contraceptives increases breast cancer risk by 25%, but the risk falls after cessation of use (73). Other risk factors are environmental and dietary factors. Ionizing radiation like that one is exposed to during x-rays can increase the risk of breast cancer, as mammary tissue is very susceptible to malignant transformation from radiation (73). Also, dietary factors such as high-fat diets, smoking, and increased alcohol intake can increase the risk of developing breast cancer (72, 73). There are also multiple germline mutations that can increase the risk of breast cancer which will be discussed in more detail below.

Carcinomas are the most common type of breast cancer (62). Carcinomas develop in the cells that line the body and organs; they are cancers of the epithelial cells. Most often, breast cancer begins in the milk-producing ducts of the breasts, which is called invasive ductal carcinoma (20). There are six key genes that contribute to the characteristics of breast carcinoma. These are the estrogen receptor (ER), the progesterone receptor (PR), the retinoic acid receptor,

the epidermal growth factor receptor family members, *p53*, and *BRCA1/BRCA2*. The first three are steroid hormone receptors (63). These include the estrogen receptor (*ER*) gene, the progesterone receptor (*PR*) gene, and the retinoic acid receptor (*RAR*).

The *ER* gene encodes the estrogen receptor (64). The effects of the *ER* receptor are mediated by the *ER* proteins, *ER- α* and *ER- β* . In the absence of estrogen, *ER- α* and *ER- β* form an inactive complex with HSP 90. When *ER* is activated, the proteins dimerize and autophosphorylate, activating themselves. Active ER can regulate gene transcription by activating the mitogen-activated protein kinase pathway (MAPK) (63). This pathway regulates cell division (65). Therefore, carcinomas that are *ER*-positive are often associated with a better prognosis because tumors tend to grow slowly. However, some breast carcinoma patients lack the *ER* gene. It is typically lost due to mutations, deletions, loss of heterozygosity, or polymorphisms in the gene. When tumors are *ER*-negative, cells grow uncontrollably and tumors are not regulated. These tumors rarely respond to endocrine therapy and are associated with poor prognosis (63). Similarly, the *PR* gene encodes the progesterone receptor (66). It has two isoforms (*PRA* and *PRB*), both of which are typically highly expressed in normal tissues, but *PRB* concentration is typically elevated in breast carcinoma. This leads to a decrease in the *PRA:PRB* ratio, which is a crucial parameter in progesterone-mediated functions such as transcription regulation (63, 67). *PR* status is a good predictor of tumor responsiveness; 75% of *PR*-positive tumors respond to endocrine therapy. Lacking the *PR* receptor typically results in a poor prognosis. The final steroid hormone receptor is the retinoic acid receptor (*RAR*). There are three variants expressed at high levels in normal tissues which regulate gene transcription. *RAR* is a tumor suppressor gene, as it inhibits cell proliferation, induces cell division, inhibits

apoptosis, and inhibits the cell cycle. Loss of the *RAR*, especially the *RAR-β* gene, is an active area of research as it is found in primary tumors (63).

The epidermal growth factor (EGF) receptor family is another set of genes typically found to be mutated in breast carcinoma. There are many genes in this family that are involved in normal mammary development. However, there are two specific genes that are found to play a role in neoplastic transformation. The HER and *erbB* proteins, which are members of the receptor tyrosine kinase family, are overexpressed in 25% of invasive breast cancer tumors (63). This is due to the fact that overexpressed HER and *erbB*, especially HER2/*erbB2*, lead to gene amplification which promotes cell proliferation and inhibits apoptosis (68).

The last two genes involved in breast carcinoma are tumor suppressor genes. The first is *p53* (63). *p53*, as stated previously, is a tumor suppressor gene that controls cell division and cell death (69). *p53* mutations are observed in 20-30% of breast carcinomas. Tumors that have *p53* mutations are more likely to be invasive, poorly differentiated, high-grade breast tumors. *p53* mutations are biomarkers for predicting cancer risk; *p53* mutations can precede the development of malignant tumors but indicate to doctors that cancer will become more aggressive. Inherited *p53* mutations that are present in Li-Fraumeni syndrome also increase the risk of breast cancer development. Li-Fraumeni syndrome is characterized by a high rate of early-onset tumors such as breast carcinoma. *p53* mutations are seen in nearly 60% of families with this disease, suggesting it is a key mutation involved in the development of carcinomas (63). Finally, *BRCA1* and *BRCA2* are key genes involved in breast carcinoma development. While hereditary breast carcinoma is rare, germline mutations in *BRCA* genes have been implicated in a high proportion of cases. *BRCA* genes regulate DNA repair and gene transcription to maintain genomic integrity;

women with a mutation in *BRCA* genes are 60 to 80% more likely to develop breast carcinoma (63).

Triple-negative breast cancer is characterized by three of these mutations. They are typically ER-negative, PR-negative, and have HER2 that is attenuated or not expressed. They are typically the most aggressive of breast cancers and have a poor prognosis because there is a lack of targeted therapies for these tumors (22). MDA-MB-231 (MDA), the breast cancer line used in this study, is triple-negative breast cancer. It was derived from a metastatic mammary adenocarcinoma from a 51-year-old caucasian female (70). The cell line has chromosomal cell counts that are nearly triploid (possessing an extra set of chromosomes) and lacks chromosomes N8 and N15 (31). MDA has mutations in *p53*, *ER*, *PR*, and *HER2*, as discussed above, as well as a number of genes discussed further below (71).

Of the mutations that occur in MDA, there were 10 preferentially essential genes that have the lowest mean subtracted score of the cell line. Like with the HeLa cell line, these genes were the most essential in causing carcinogenic growth (74). The first was *NAMPT*, which catalyzes the synthesis of *NAD*, which is known to mediate inflammation, a marker of cancerous development (75). Next was the *WDR73* gene, which, when reduced in expression, results in abnormalities in the size and morphology of the nucleus, which is characteristic of cancerous cells (76). *SNRPB2* was also mutated and has been known to play a role in pre-mRNA splicing (77). The *UBIADI* gene, which has been known to play a role in phospholipid metabolism, was also mutated (78). Inefficient phospholipid metabolism in the cell can lead to misshapen cancerous cells. The *PELO* gene was also mutated. This gene plays a role in cell cycle control and cell division (79). Having a mutation in the *PELO* gene can lead to dysregulation of the cell cycle and uncontrolled cellular division. The *BRATI* is a *BRCA1* and *ATM-associated* gene.

These genes work together to control the cell cycle checkpoints required for DNA damage repair (80). Mutations in this gene lead to dysregulation of the cell cycle and potential replication of mutations. The *ADSS2* gene is involved in the conversion of inosine monophosphate to adenosine monophosphate, which has been known to speed healing (81, 82) Having mutations in this gene can lead to a lack of healing and errors in cells. The *SLC4A7* gene is a transmembrane protein that is known to transport sodium and bicarbonate to regulate intracellular pH (83). It is often found to be downregulated in tumors. Mutations typically increase the risk of cancer, especially breast cancer (84). The *RAB7A* gene regulates vesicle traffic into endosomes and lysosomes, and mutations result in a lack of waste degradation (85). Finally, the *ELMO2* gene functions in cell migration and apoptosis, and mutations lead to metastasis and cells evading death (86).

Table 2: A list of the major genes mutated in MDA cells, their function, and how a mutation in that gene can lead to cancerous growth.

Gene	Function	Mutation
<i>NAMPT</i>	Catalyzes the synthesis of <i>NAD</i> , a mediator of inflammation	Increased inflammation
<i>WDR73</i>	Regulates the shape and morphology of the nucleus	When reduced in expression, results in abnormalities in the size and morphology of the nucleus
<i>SNRPB2</i>	pre-mRNA splicing	Dysregulation of mRNA splicing (improper removal of introns)
<i>UBIAD1</i>	Phospholipid metabolism	Build up of waste; improper regulation of the cell membrane; misshapen cells
<i>PELO</i>	Controls cell cycle and cell division	Dysregulation of cell cycle (cells divide when they aren't supposed to) and cell division (hyperplasia)

<i>BRAT1</i>	Cell cycle control	Dysregulation of cell cycle
<i>ADSS2</i>	Conversion of inosine monophosphate to adenosine monophosphate	Improper healing
<i>SLCAA7</i>	Transports sodium and bicarbonate to regulate intracellular pH	Unknown; often downregulated in tumors
<i>RAB7A</i>	Regulates vesicle traffic into endosomes and lysosomes	Waste buildup
<i>ELMO2</i>	Cell migration and regulating apoptosis	Metastasis, avoidance of apoptosis

Methods

Materials

In this study, the breast cancer cell line used was MCF7. The line is a triple-negative cell line. It was isolated from a 69-year-old female at the primary site (breast, mammary gland). The cells are epithelial and come from a breast adenocarcinoma (31). The cervical cancer cell line used was HeLa. HeLa cells were isolated from a 31-year-old African American woman. The cells came from uterine and cervical tissue. They were epithelial and originated from a cervical adenocarcinoma caused by HPV infection (32).

Cell Culture

Frozen HeLa and MCF7 cells were thawed by removing the vial from the -80°C storage freezer and placing the lower half of the vial in the 37°C water bath. The cells thawed for 1-2 minutes. They were removed from their vial and diluted in media in a 50 mL centrifuge tube. The cells were centrifuged to remove the remaining dimethyl sulfoxide (DMSO). The cells were then placed in a labeled culture flask. In 10 mL of growth media, containing either EMEM or DMEM/F-12 in a 50-50 split, the cells were pipetted into the culture flask. The cells were

incubated at 37°C and 5% CO₂. Every two to three days, the old media was removed from the flask, and 8 mL of new media was added to the flask.

When the cells were 80-90% confluent, they were split. First, the old media was removed from the flask. Then, the cells were washed with 5 mL of Phosphate-buffered saline (PBS). Once the PBS was removed, 3 mL of trypsin was added to the flask. The flasks were returned to the incubator. Once all of the cells were detached from the flask (3 to 5 minutes), an equal amount of media (3 mL) was added to the flask to deactivate the trypsin. This solution was then transferred to a centrifuge tube. The cells were centrifuged at 2000 RPM for 8 minutes. Once the centrifuge was completed, the supernatant was removed. The cells were vortexed to dislodge them from the bottom of the tube. The cells were then pipetted out of the centrifuge tube and divided equally between three flasks, completing the 1:3 split. The cells were refed with 8 mL of media and returned to the incubator. This process was identical for both HeLa and MCF7 cells.

Cell Pellet Construction

To run the speed of sound and attenuation experiments, the cancer cells had to be made into a cell pellet since in this form a reliable ultrasound can be performed. First, the cells had to be counted. Once the cells were confluent enough (about 80-90%), they were detached from the flask and counted. The old media was removed, and cells were washed with 5 mL PBS. The PBS was then removed and 3.0 mL of trypsin was added to the cells. They were then incubated for five minutes at 37°C and 5% CO₂. Once the cells were no longer attached to the flask, an equal amount of media (3.0 mL) was added to the flask. The solution was removed from the flask and placed in a centrifuge tube. A 100 µL sample was taken and added to an Eppendorf tube. 100 µL of trypan blue was added, and they were mixed using the pipette. Next, about 10 µL of the sample was added to the hemocytometer. The coverslip was sealed using a small amount of

water, and the samples filled both wells of the hemocytometer. The number of live and dead cells was counted under the microscope. The overall number of live and dead cells in the sample was calculated in excel. This study aimed for a cell density of about 5 million cells/mL. This information was necessary for constructing the cell pellet so that the cell density of the pellet was known and could be recreated in every experiment.

There were two parts to the cell pellet: the holder and the cell pellet itself. The cell pellet was constructed by cutting a centrifuge tube to create a hollow cylinder. Saran wrap was placed on the bottom to close one side. To create the cell pellet, live cells were suspended in an agar solution (Figure 5). The known number of viable cells in the centrifuge tube was centrifuged for 8 minutes at 2000 RPM. All but 1 mL of the supernatant was removed and then the cells were resuspended in the media using a vortex. Then, 1 mL of agar was added to the cells in the centrifuge tube. The agar and cells were transferred to the cell pellet holder and allowed to harden. The top of the pellet was sealed with saran wrap and secured with rubber bands.



Figure 5: An image of a completed cell pellet, including the agar sample, holder, saran wrap, and elastics. The pellet appears pink due to the color of the media.

Experiment

The speed of sound and attenuation are measured using a narrow band, through a transmission experimental setup. There were two transducers that share the same center frequency; one, the transmitter, sends the signal, and the other, the receiver, receives the signal. There were three pairs of transducers used with different center frequencies; 5 MHz, 10 MHz, and 15 MHz. Between the transducers was the cell pellet held inside a stand. The transducers are lowered into a deionized water bath held at about 30°C. For some tests of the MDA cells, due to temperature regulation issues, the temperature was as low as 23°C.

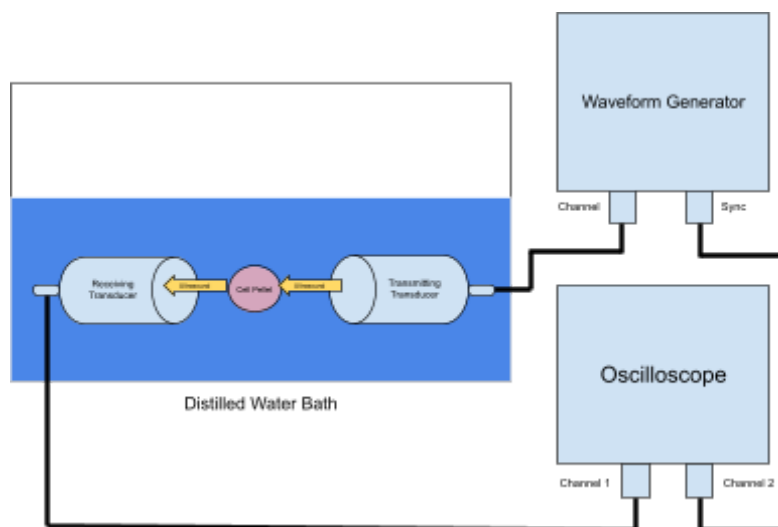


Figure 6: Set-up of the speed of sound and attenuation experiment.

Before data collection could begin, it was necessary to ensure the surfaces of the transducers were parallel to ensure they had the same center frequency. This was done by adjusting the angles of the transducers and using the computer program, COSMOS, to move one of the transducers in various directions. The alignment of the transducers was delineated by the amplitude of the waveform on the oscilloscope. The higher the amplitude of the waveform, the

closer the transducers are to parallel. Once the amplitude was at its maximum, the transducers were parallel, and the experiment could proceed.

For data collection, a waveform generator and an oscilloscope were used. A waveform generator (Aligent 33500B) sent a signal frequency sine pulse over the bandwidth of the transducers. Per cycle, it sent out 20 cycle bursts. The burst period was 10 ms. The waveform signal was transformed into an ultrasonic pulse by the transducer. This pulse then passed through the water, then the sample, and then the water again, to be received by the receiving transducer. The receiving transducer recorded the signal on the oscilloscope. The pulse is received by the second transducer which records it on an oscilloscope (Tectronix TDS 3014C). The peak-to-peak amplitude and the time of arrival are measured for a water path only and then for the same path but with the cell pellet.

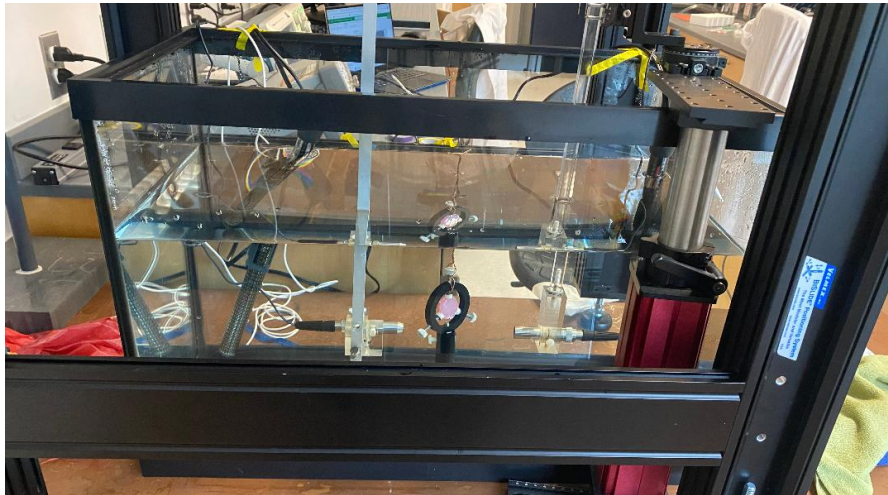


Figure 7: Side view of the speed of sound and attenuation experimental setup. The transmitting transducer is on the left and the receiving transducer is on the right. The cords attach them to the waveform generator and oscilloscope, respectively. The sample and holder are not in the path of the transducers because this represents a test of the speed of sound and attenuation of the water only.

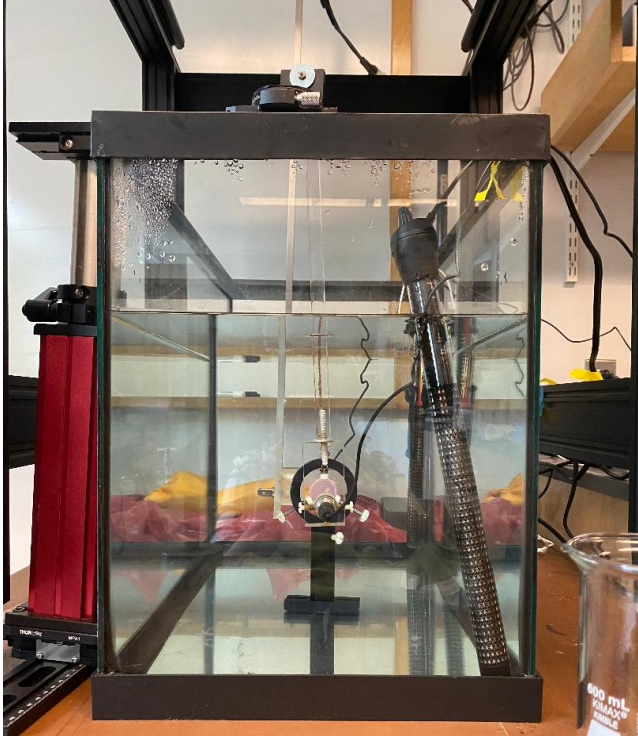


Figure 8: Front view of the speed of sound and attenuation experimental setup. The transmitting transducer is closest. The sample is between the transducer because this represents a test of the speed of sound and attenuation of the cells. The receiving transducer is behind the cell pellet and holder.

For each transducer, three sets of data were taken at each frequency per pellet to reduce random error and check for inconsistencies in the data. The 5 MHz transducers recorded data from 2 MHz to 8 MHz in 1 MHz steps. The 10 MHz transducers recorded data from 7 MHz to 12 MHz. The 15 MHz transducers recorded data from 12 MHz to 18 MHz.

Calculations

To find the speed of sound, the time it takes from the sine pulse to reach the receiving transducer with and without the same was measured. The difference between the two times is used to calculate the speed of sound in the sample. Speed of sound is found using the equation:

$$C_s = \frac{dC_w}{c_w \epsilon - \Delta t c_w}$$

c_s is the speed of sound of the sample, c_w is the speed of sound of water, d is the width of the sample, and Δt is the difference in time between the water only path and the path with the sample.

To find the attenuation, the amplitude of the water-only path is compared to the amplitude of the path with the sample inserted. The cell pellet is constructed using saran windows, so a correction for the transmission coefficient of saran is included. The transmission coefficient is:

$$T^2 = (4Z_1 Z_3)/(Z_1 + Z_3)^2 \cos^2(k_2 l) + (Z_2 + (\frac{Z_1 Z_3}{Z_2}))^2 \sin^2(k_2 l)$$

where k_2 is the wavenumber of the sine pulse, the thickness of the saran layer is l , Z_2 is the acoustic impedance of the saran, Z_1 is the acoustic impedance of the water, and Z_3 is the acoustic impedance of the sample material. The attenuation coefficient in dB/cm can then be solved using the general equation:

$$\alpha = \frac{20}{d} \log\left(\frac{A_w}{A_s} T^2\right)$$

where A_w is the amplitude measured for the water path and A_s is the amplitude measured with the sample in the path.

Results

Concentration

Approximately 5 million cells were used per cell pellet, regardless of cell type. In practice, the actual cell concentration was between 4.5 million and 5.5 million. The approximate cell count was calculated in excel by multiplying the total live cells from the cell count by the flask area and dilution factor of cells to agar. A summary of the cell count for the HeLa and

MDA experiments are seen below in Tables 3 and 4, respectively. Except for experiment #1, all of the HeLa experiments had a cell count within the ideal limit (Table 3). All of the MDA experiments had cell counts within the ideal limit (Table 4).

Table 3: Cell concentration summary for the five HeLa cell experiments.

Experiment #	Cell Count
1	6,780,000
2	5,150,000
3	5,413,333
4	5,316,666
5	5,320,000

Table 4: Cell concentration summary for the four MDA cell experiments.

Experiment #	Cell Count
1	5,130,000
2	5,126,666
3	4,626,666
4	4,570,000

Speed of Sound

The average speed of sound for the HeLa cells was calculated by averaging all of the results from each of the trials. Further, the average speed of sound of the HeLa cells was 1527.6 ± 3.1 m/s, as summarized below in Table 5.

Table 5: A summary of the average speed of sound for each transducer and the average overall speed of sound for the HeLa cell experiments.

Transducer (MHz)	Average Speed of Sound (m/s)
5	1525.6 ± 3.1

10	1529.3±2.9
15	1528±3
Average	1527.6±3.1

The average speed of sound for the MDA cells was calculated in three ways. First, the average result of all of the trials was found. Across all the trials, the average speed of sound was 1518.5 ± 3.4 m/s. However, since the first two trials and the second two trials had such a difference in temperature (23°C vs. 30°C) an average speed of sound was also found for the “cold” trials (23°C) and the “hot” trials (30°C). Further, the average speed of sound for the cold trials was 1509.5 ± 2.8 m/s and the average speed of sound for the hot trials was 1527.5 ± 3.9 m/s. All of these data are summarized below in Table 6.

Table 6: A summary of the average speed of sound for each transducer and the average overall speed of sound for the MDA cell experiments; the first section, titled “All”, represents the overall speed of sound, the second section, titled “Cold” represents the speed of sound for the cold experiments, and the final section, titled “Hot” represents the speed of sound for the hot experiments.

Temperature ($^{\circ}\text{C}$)	Transducer (MHz)	Average Speed of Sound (m/s)
All		
	5	1518.0±4.1
	10	1516.5±2.9
	15	1521.5±3.1
	Average	1518.5±3.4
Cold		
	5	1509.7±3.7
	10	1508±2
	15	1510.9±2.6

	Average	1509.5±2.8
Hot		
	5	1526.2±4.5
	10	1525.0±3.7
	15	1531.4±3.6
	Average	1527.5±3.9

Attenuation

The attenuation of the HeLa and MDA cells are graphed below in Figure 9. This figure includes the average attenuation of the cells in a range of 2 to 18 MHz. Both the HeLa cells and the MDA cells showed increasing attenuation with increasing frequency. The HeLa cells on average had smaller attenuation than the MDA cells. However, the MDA cells had larger error at high frequencies. A p-test of the data yielded 0.000501 at a significance level of $\alpha = 0.05$, suggesting there is no difference in the data. Deviance calculations support this conclusion, but the deviance increased as frequency increased, suggesting attenuation does increase with frequency for MDA cells.

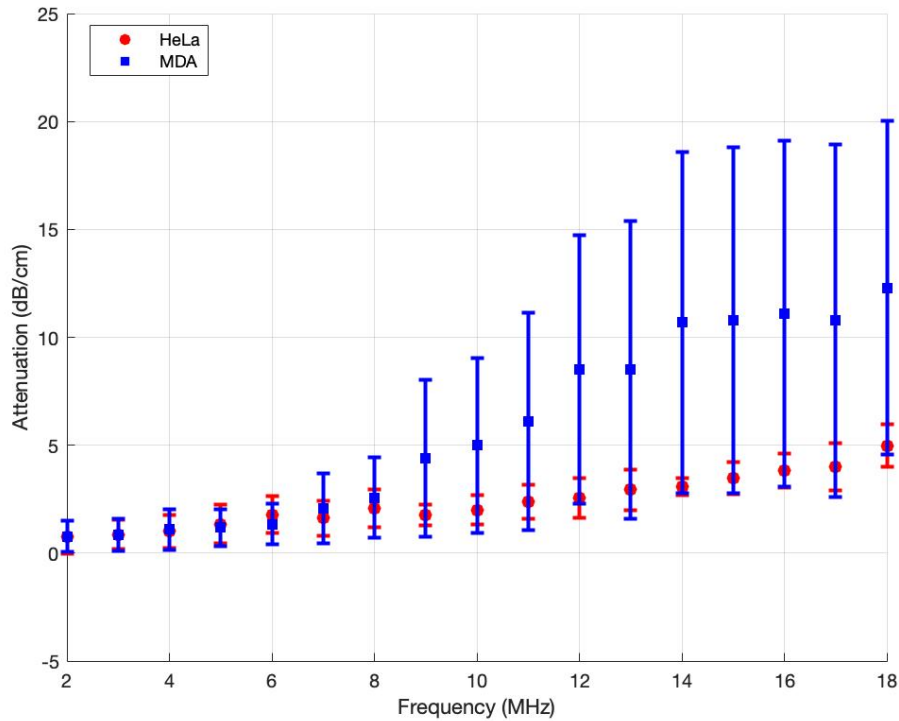


Figure 9: A graph of the attenuation of the MDA cells and HeLa cells, with the MDA cells in blue and the HeLa cells in red.

Table 5 is a table of direct comparison of the data. It summarizes the data from the entire experiment. The average density of the cell pellets for HeLa and MDA cells are in the first column; while they did vary, they were about within half a million of 5 million cells. The average speed of sound was calculated above; comparison was made between the HeLa cells and the hot MDA experiments to keep variables constant. Finally, the average attenuation coefficient per frequency was calculated. This coefficient was much higher for MDA cells, suggesting MDA cells have a higher attenuation response with a stronger frequency power dependence.

Table 7: A table of direct comparison of all of the data. The average density was calculated using the data in Tables 3 and 4 and taking the average of them. The average speed of sound was found above in Tables 5 and 6. The attenuation coefficient was found by dividing the attenuation at each frequency by that frequency and taking the average of that value.

Cell Type	Average Density	Speed of Sound, m/s	Attenuation Coefficient, dB/MHz
HeLa	5,595,999	1527.6±3.1	0.25±0.04
MDA	4,863,333	1527.5±3.9	0.5±0.2

Discussion

Speed of Sound - Analysis

As stated previously, the average speed of sound for all temperatures of the HeLa cells was 1527.6±3.1 m/s. The average speed of sound for all temperatures for the MDA cells was 1518.5±3.4 m/s. However, variation in temperature for the MDA tests suggests that the speed of sound is temperature dependent, as expected. At low temperatures, the average speed of sound was 1509.5±2.8 m/s, but at high temperatures, the average speed of sound was 1527.5±3.9 m/s. There is a large difference between these values and the error in the calculations does not rectify them, showing that the speed of sound is temperature-dependent. Multiple studies have previously exemplified the temperature dependence of the speed of sound in both water and human tissue. Specifically, Kumar et al. determined that the speed of sound increases with increasing temperature before reaching a thermal maximum at 75°C, and Bamber and Hill determined that the speed of sound for non-fatty human tissues (such as cancerous masses) increases with temperature and reaches a maximum at 50°C (86. 87). Therefore, due to the significant difference in the speed of sound data for the MDA cells at different temperatures and the temperature dependence of the speed of sound in both water and tissue, the speed of sound

for hot temperatures will be used to compare to HeLa cells since hot temperatures were used for all of the HeLa tests.

Comparing the speed of sound of HeLa cells, 1527.6 ± 3.1 m/s, and the speed of sound of MDA cells at hot temperatures, 1527.5 ± 3.9 m/s, one observes there is no difference in speed of sound between the two cell types. While the difference in mutations discussed above would suggest there would be a difference in the speed of sound between HeLa and MDA cells, there are multiple reasons why this was not the case experimentally. First, since the speed of sound typically relies on density, a lack of variation in the density of the cell pellets could explain the similar speed of sounds. Although the concentration of cells varied between tests, it always remained within the range of $5.0 \times 10^9 \pm 10^9$ cells, and the density of all of the cell pellets remained similar in all of the tests (between 0.9 and 0.94 g/cm³). This could explain the lack of variation in the speed of sound results for the different cancer types.

Molecularly, the lack of difference in the speed of sound between HeLa and MDA cells could be due to the morphology of cancer cells. To metastasize, all epithelial cells must detach from the original tumor and breach the basement membrane to invade neighboring tissues. The cells typically acquire a spindle-shaped morphology and enhance migration (88). Both HeLa cells and MDA cells originate from epithelial tumors, which means their initial stage of metastasis was the same, even if the mutations acquired to get there were not the same. For example, some of the mutations in HeLa cells that led to metastasis include the *E6* protein affecting *paxillin*, which leads to the rupture of the cytoskeleton and cellular invasion as well as *TNS2*, which regulates invasion and metastasis. In MDA cells, the mutation of *ELMO2* results in metastasis. Therefore, although the mutations acquired leading to metastasis and therefore a change in morphology of cells are not the same between MDA and HeLa cells, since they are

both epithelial cells and the mechanism of metastasis is the same, it follows that they could have similar morphology which leads to similar propagation of sound waves.

Further, although all types of cancerous cells typically have varying morphology, they usually have similar mutations leading to aneuploidy, nuclear membrane irregularities, and dysplasia (89). For example, in MDA cells, mutations in *WDR73* and *UBIADI* result in abnormal nuclei and membrane morphology. Therefore, the morphological features of different cancer types are more similar than that of normal and malignant cells. This could explain why studies such as the study performed by Doyle *et al.* have found a difference in the speed of sound in normal and malignant cells and this study did not show differences in malignant cells.

Attenuation - Analysis

As seen in Figure 5, the HeLa cells on average had smaller attenuation than the MDA cells. However, the error for both types of cells makes it impossible to conclusively determine any difference. As stated previously, attenuation is the decay rate of a wave as it moves through a material. The higher the attenuation is, the more distorted a wave becomes, suggesting that lower attenuation means the wave was transmitted more effectively. Both relationships can be examined physically and molecularly.

The smaller attenuation of the HeLa cells than the MDA cells, especially at higher frequencies, suggests that the HeLa cells transmitted the wave more effectively than the MDA cells. Since the distance between the transducers remained relatively similar between the trials, the increase in attenuation seen in the MDA tests was likely due to interference. This could be due to the characteristics of the MDA cells; it is possible mutations in the cell cause it to scatter waves and absorb the energy differently. For example, as stated above, mutations in *WDR73* and *UBIADI* result in abnormal cell and nucleus morphology. This could make cancerous cells

interact with sound waves more than the HeLa cells. Other potential explanations for the higher attenuation of the MDA cells include clumps in the cell pellet, debris in the water, or, potentially, underlying infection. Bacterial infection was common throughout the length of writing this thesis; infection recurred multiple times over the course of the four months the experiments were completed. This necessitated taking data with infected cells, which was not included in this thesis but implied that the infection affected the results of the experiment. Although the MDA cells appeared clear of infection at the time of testing, it is possible that an infection was present which increased interference in the test and resulted in a higher attenuation.

Due to the large error in the MDA tests, it is possible that the attenuation did not vary between the MDA and HeLa cells. This is supported by the results of the p-test and the deviation calculations. This could be because, as stated previously, since these were both cancerous cell lines and neither was non-cancerous, they had similar morphologies that lead to interference with similar attenuation values. Both HeLa cells and MDA cells have mutations that lead to dysplasia, rapid cell division, and metastasis. Specific mutations that lead to abnormal morphology in MDA cells are loss of the *ER* receptor, loss of the *RAR* gene, overexpressed HER and *erbB*, and *p53*, *WDR73*, *UBIADI1*, *PELO*, and *BRAT1* mutations. Further, specific mutations that lead to abnormal morphology in HeLa cells are *E6* and *E7* activation and *CRNKLI*, *NOL7*, *GNRHI*, and *DCTN6* mutations. As seen above, although these mutations are not identical, they either affect similar pathways or have similar consequences that lead to the altered morphology of cancerous cells. This altered morphology could result in interference that leads to similar attenuation values among MDA and HeLa cells.

There is not enough evidence in this experiment to determine if there was a difference in attenuation between MDA and HeLa cells. While the p-test and discrepancy calculations suggest

there is no difference, the average attenuation coefficient per frequency suggests otherwise. The average attenuation coefficient per frequency of HeLa cells was 0.25 ± 0.04 dB/MHz, and the average attenuation coefficient per frequency of the MDA cells was 0.5 ± 0.2 dB/MHz. This suggests the MDA cells transmit the waves more effectively than HeLa cells. Taken with the discrepancy calculations, which increased at higher frequencies, it is possible that the MDA cells do have higher attenuation responses at higher frequencies. However, further research must be done to confirm this.

Future Research

Further research could be done to examine the results of this study, particularly in regard to the attenuation results. The larger error bars in the MDA attenuation data were unavoidable because of the unpredictable nature of the data, but time constraints prevented another data set from being recorded. Taking further MDA data could help refine the data that were recorded to decrease the error bars and prove if there is a difference in attenuation between MDA cells and HeLa cells.

Physically, there are multiple other experiments that could be done as a follow-up to this study. One could examine the speed of sound and attenuation data of other types of cancer to see if they differ from cervical and breast cancer to determine if it is possible to distinguish between cancer types via ultrasound. One could also examine other characteristics of these two cell lines, such as backscatter, to see if other characteristics could be used to distinguish between them. Backscatter coefficients could give further information about morphology differences by giving information about scatter size. Biologically, it is also possible to design other experiments to support the conclusions of this study. Specifically, one could examine some of the major proteins expressed by the two cell lines to determine if the expression actually impacts morphology and

explains why the results were similar. This could prove if the cells were actually morphologically similar or if the mutations in the cells resulted in very different tumors and therefore the similarities in the speed of sound and attenuation were due to other causes.

Conclusions

The results of this study show no measured difference in the tissue characteristics of the speed of sound between MDA and HeLa cells, and further experiments are needed to determine if there is a potential difference in the attenuation between MDA and HeLa cells. Therefore, this study does not propose a definitive way to ultrasonically differentiate between breast and cervical cancer cells. This could have been due to the density similarities in the cell pellets or morphological similarities between cancerous cells due to the nature of cancer cells. Further research should be done to validate the conclusions of this study, determine if other types of cancer differ from breast and cervical cancer and can be diagnosed via ultrasound, and if the proteins expressed in these cell lines resulted in cancerous morphologies that explain the similarities or if the similarities are due to other reasons. The conclusions of this study and future research that could be done as an extension would be particularly beneficial in helping diagnose metastasized tumors. For example, if the original site of metastasis is unknown for a tumor, developing a database of quantitative ultrasound characteristics for various cell types would allow doctors to not just diagnose cancer, but also find the source of the cancer and treat it accordingly.

References

- (1) Siegel, Rebecca; Miller, Kimberly; Jemal, Ahmedin. "Cancer Facts & Figures 2022." *American Cancer Society*. 12 January 2022.
<https://www.cancer.org/research/cancer-facts-statistics/all-cancer-facts-figures/cancer-facts-figures-2022.html>. Accessed 29 June 2022.
- (2) "Cancer Statistics." *National Cancer Institute*.
<https://www.cancer.gov/about-cancer/understanding/statistics>. Accessed 29 June 2022.
- (3) Weir, Hannah; Thompson, Trever; Stewart, Sherri; White, Mary. "Cancer Incidence and Projections in the United States Between 2015 and 2050." *Preventing Chronic Disease*, Volume 8.
https://www.cdc.gov/pcd/issues/2021/21_0006.htm#:~:text=Because%20of%20the%20growth%20and,adults%20aged%20%E2%89%A575%20years.
- (4) "Cancer Blood Tests: Lab Tests Used in Cancer Diagnosis." *Mayo Clinic*. 2022.
<https://www.mayoclinic.org/diseases-conditions/cancer/in-depth/cancer-diagnosis/art-20046459#:~:text=Some%20blood%20tests%20used%20to,be%20found%20using%20this%20test>. Accessed 29 June 2022.
- (5) "Imaging (Radiology) Tests for Cancer." *American Cancer Society*. 2022.
<https://www.cancer.org/treatment/understanding-your-diagnosis/tests/imaging-radiology-tests-for-cancer.html>. Accessed 29 June 2022.
- (6) "How Cancer is Diagnosed." *National Cancer Institute*. Updated 19 July 2017.
<https://www.cancer.gov/about-cancer/diagnosis-staging/diagnosis>. Accessed 29 June 2022.
- (7) "Biopsy." *Cancer.net*. Approved October 2021.
<https://www.cancer.net/navigating-cancer-care/diagnosing-cancer/tests-and-procedures/biopsy>. Accessed 29 June 2022.
- (8) Feleppa Ernest; Mamou, Jonathan; Porter, Christopher R. Machi, Junji. "Quantitative Ultrasound in Cancer Imaging." *Semin Oncology*, Volume 38, Issue 1, pages 136-150, 2011. <https://www.ncbi.nlm.nih.gov/pmc/articles/PMC3057450/>.
- (9) "General Ultrasound." *RadiologyInfo.org*. Reviewed 15 June 2020.
<https://www.radiologyinfo.org/en/info/genus>. Accessed 29 June 2022.
- (10) O'Brien, William. "A Temporal View of Soft Tissue Quantitative Ultrasound." *Physics Procedia*, Volume 70, pages 1127-1130, 2015.
- (11) Chiavacci, Iacopo. "Propagation Speed." *Radiopaedia.org*. Revised 02 August 2021.
<https://radiopaedia.org/articles/propagation-speed?lang=us#:~:text=The%20propagation%20speed%20of%20sound,m%2Fsec%20through%20tissue%201.&text=The%20propagation%20speed%20of%20sound%20is%20higher%20in%20tissues.stiffness%20and%20reduced%20density2>
- (12) Hooi, Fong Ming; Kripfgans, Oliver; Carson, Paul L.. "Acoustic attenuation imaging of tissue bulk properties with a priori information." *The Journal of Acoustical Society of America*, Volume 140, Issue 3, pages 2113-2122.
<https://www.ncbi.nlm.nih.gov/pmc/articles/PMC5114017/>.
- (13) O'Brien, William; Oelze, Michael; Han, Aiguo. "Tissue Characterization Through Ultrasonic Backscatter." *Bioacoustics Research Lab*.
https://www.brl.uiuc.edu/Projects/tissue_characterization_through_ultrasonic_backscatter.php

- (14) Teisseire, Maxime; Han, Aiguo; Abuhabsah, Rami; Blue Jr., James P.; Sarwate, Sandhya; O'Brien Jr, William D. "Ultrasonic Backscatter Coefficient Quantitative Estimates from Chinese Hamster Ovary Cell Pellet Biophantoms." *The Journal of the Acoustical Society of America*, Volume 128, 3175-80. Nov 2010.
<https://pubmed.ncbi.nlm.nih.gov/21110612>.
- (15) Doyle, Timothy; Goodrich, Jeffery; Ambrose, Brady J.; Patel, Hemang; Kwon, Soonjol; Pearson, Lee H. "Ultrasonic Differentiation of Normal Versus Malignant Breast Epithelial Cells in Monolayer Cultures." *The Journal of the Acoustical Society of America*, Volume 128 (5). Nov 2010.
- (16) "Worldwide Cancer Data." *World Cancer Research Fund International*. Last accessed 23 March 2022. <https://www.wcrf.org/cancer-trends/worldwide-cancer-data/>
- (17) Kaminska et al. "Breast Cancer Risk Factors." *Prz Menopauzalny*, Volume 14, Issue 3, pages 196-202. <https://www.ncbi.nlm.nih.gov/pmc/articles/PMC4612558/>
- (18) Sung et al. "Global Cancer Statistics 2020: GLOBOCAN Estimates of Incidence and Mortality Worldwide for 36 Cancers in 185 Countries. *CA: A Cancer Journal for Clinicians*, Volume 71, Issue 8, pages 209-245.
<https://acsjournals.onlinelibrary.wiley.com/doi/10.3322/caac.21660>
- (19) "Cervix Statistics." *American Cancer Society*.
<https://cancerstatisticscenter.cancer.org/#!/cancer-site/Cervix>
- (20) "Breast Cancer." *Mayo Clinic*. 2022.
<https://www.mayoclinic.org/diseases-conditions/breast-cancer/symptoms-causes/syc-20352470>
- (21) Walks, Adrienne; Winer, Eric. "Breast Cancer Treatment: A Review." *Clinical Review and Education*, Volum 321, Number 3, pages 288-300.
<http://bdrc.tums.ac.ir/uploads/140/2020/Jun/17/Breast-Cancer-Treatment-Jan-2019-1.pdf>
- (22) Carey, Lisa; Irvin, William. "What is Triple-Negative Breast Cancer?" *European Journal of Cancer*, Volume 44, Issue 18, pages 2799-2805.
https://www.sciencedirect.com/science/article/pii/S0959804908007508?casa_token=cd8S15lfom0AAAAA:S9vZUOaqNgxR2gTvaLOejLKE1YFQvBP5uCvzy-CXUU1IVjO-WUL9ZrSPGbjJ8Hh1P9xsZXzndg
- (23) Chacon, Reinaldo; Costanzo, Maria. "Triple-Negative Breast Cancer." *Breast Cancer Research*, Volume 12, Supplement 2.
<https://breast-cancer-research.biomedcentral.com/articles/10.1186/bcr2574>
- (24) Nokoane, Lerato. "Triple-Negative Breast Cancer." *PathChat*, Edition no. 33.
<https://www.ampath.co.za/pdfs/ampathchats/pathchat-33-triple-negative-breast-cancer.pdf>
- (25) "Mammogram Basics." *American Cancer Society*. Revised 14 January 2022.
<https://www.cancer.org/cancer/breast-cancer/screening-tests-and-early-detection/mammograms/mammogram-basics.html>
- (26) "Triple-negative Breast Cancer. *American Cancer Society*. Revised 1 March 2022.
<https://www.cancer.org/cancer/breast-cancer/about/types-of-breast-cancer/triple-negative.html>
- (27) Oyervides-Munoz et al. "Understanding the HPV Integration and its Progression to Cervical Cancer." *Infection, Genetics and Evolution*, Volume 61, pages 134-144.
https://www.sciencedirect.com/science/article/pii/S156713481830090X?casa_token=M

- [UZZRmUeC4AAAAA:VcBL1FP4sssnIf0vqotyFSFCmA3mS8R6IFPV0C5rmqxwodvuRVv6izSbWztOdrQjiNXpifdsg](https://www.sciencedirect.com/science/article/pii/S014067361832470X?casa_token=FtCB8r0xVkIAAAAA:mFkT3BbKpk7Q3vGuhxNPq87QFOHsJ1CO7ZC50tR22vw6rdJ3Fz5otLw9xOih5PYdwh_-YovSBQ)
- (28) Cohen et al. “Cervical Cancer.” *The Lancet*, Volume 393, Issue 10167, pages 169-182.
https://www.sciencedirect.com/science/article/pii/S014067361832470X?casa_token=FtCB8r0xVkIAAAAA:mFkT3BbKpk7Q3vGuhxNPq87QFOHsJ1CO7ZC50tR22vw6rdJ3Fz5otLw9xOih5PYdwh_-YovSBQ
- (29) de Freitas et al. “Susceptibility to Cervical Cancer: An Overview.” *Gynecologic Oncology*, Volume 126, Issue 2, pages 304-311.
<https://www.sciencedirect.com/science/article/pii/S009082581200248X>
- (30) “Cervical Cancer Screening.” *The American College of Obstetricians and Gynecologists*. 2022.
<https://www.acog.org/womens-health/faqs/cervical-cancer-screening#:~:text=Cervical%20Cytology%3A%20The%20study%20of%20an%20instrument%20called%20a%20colposcope>.
- (31) “MCF7.” ATCC. 2022. <https://www.atcc.org/products/htb-22>
- (32) “HeLa.” ATCC. 2022. <https://www.atcc.org/products/crm-ccl-2>
- (33) “Cancer.” The Mayo Clinic.
<https://www.mayoclinic.org/diseases-conditions/cancer/symptoms-causes/syc-20370588>
- (34) Chial, Heidi. “Proto-oncogenes to Oncogenes to Cancer.” *Nature Education* Volume 1, Issue 1, page 33.
<https://www.nature.com/scitable/topicpage/proto-oncogenes-to-oncogenes-to-cancer-883/>
- (35) Rajasekaran, N.; Shin, Y.K.; Wang, L.H.; Wu, C. F. “Loss of Tumor Suppressor Gene Function in Human Cancer: An Overview.” *Cell Physiol Biochem*, 2018, Volume 51, pages 2647-2693. <https://www.karger.com/Article/FullText/495956>
- (36) Oyervides-Munoz et al. “Understanding the HPV Integration and its Progression to Cervical Cancer.” *Infection, Genetics and Evolution*, Volume 61, pages 134-144.
https://www.sciencedirect.com/science/article/pii/S156713481830090X?casa_token=MUZZRmUeC4AAAAA:VcBL1FP4sssnIf0vqotyFSFCmA3mS8R6IFPV0C5rmqxwodvuRVv6izSbWztOdrQjiNXpifdsg
- (37) Waggoner, Steven. “Cervical Cancer.” *The Lancet*, Volume 316, Issue 9376, 28 June 2003, pages 2217-2225.
https://www.sciencedirect.com/science/article/pii/S0140673603137786?casa_token=1LiJPpJlZjwAAAAA:geyF9YyuehxkmarDTLu85Kd9fClj8n6xvpQpmDQjrP--VEpPJ_7DHmRlnQ3SRNGWLq3S99mfk
- (38) “Cervical Cancer.” The Mayo Clinic.
<https://www.mayoclinic.org/diseases-conditions/cervical-cancer/symptoms-causes/syc-20352501#:~:text=The%20main%20types%20of%20cervical,cancers%20are%20squamous%20cell%20carcinomas>
- (39) Cohen et al. “Cervical Cancer.” *The Lancet*, Volume 393, Issue 10167, pages 169-182.
https://www.sciencedirect.com/science/article/pii/S014067361832470X?casa_token=FtCB8r0xVkIAAAAA:mFkT3BbKpk7Q3vGuhxNPq87QFOHsJ1CO7ZC50tR22vw6rdJ3Fz5otLw9xOih5PYdwh_-YovSBQ
- (40) “HPV and Cancer.” National Cancer Institute. Updated 12 September 2022.
<https://www.cancer.gov/about-cancer/causes-prevention/risk/infectious-agents/hpv-and-c>

- [ancer#:~:text=There%20are%20about%2014%20high,for%20most%20HPV%2Drelated%20cancers](#)
- (41) “p53 gene.” National Cancer Institute.
<https://www.cancer.gov/publications/dictionaries/cancer-terms/def/p53-gene>
 - (42) “BAK1.” Cancer Genetics Web. Reviewed 31 August 2019.
<http://www.cancerindex.org/geneweb/BAK1.htm>
 - (43) Dominguez, Roberto; Holmes, Kenneth. “Actin Structure and Function.” *Annu Rev Biophys.* 2011 July 9, Volume 40, pages 169-186.
<https://www.ncbi.nlm.nih.gov/pmc/articles/PMC3130349/>
 - (44) de Freitas, Antonio Carlos; Gurgel, Ana Pavla Almeida Diniz; Chagas, Bárbara Simas; Coimbra, Eliane Campos; do Amaral, Carolina Maria Medeiros. “Susceptibility to Cervical Cancer: An Overview.” *Gynecologic Oncology.* Volume 126, Issue 2, August 2012, pages 304-311.
https://www.sciencedirect.com/science/article/abs/pii/S009082581200248X?casa_token=iyX8Qmh7dhoAAAAA:8nogxQZPW-L37ecx1KjdVvN7reVJI9FuTldJmFwAOB1MGGFfpPPqLEw3vAXBhbSwABNMV-06RQ
 - (45) Mata-Rocha, Minerva; Rodríguez-Hernández, Ruth Monserrat; Chávez-Olmos, Pedro; Garrido Efraín; Robles-Vázquez, Conrado; Aguilar-Ruiz, Sergio; Torres-Aguilar, Honorio; González-Torres, Carolina; Gaytan-Cervantes, Javier; Mejía-Aranguré, Juan Manuel; de los Angeles Romero-Tlalolini, María. “Presence of HPV DNA in Extracellular Vesicles from HeLa Cells and Cervical Samples.” *Enfermedades Infecciosas y Microbiología Clínica*, 2019.
https://www.researchgate.net/profile/Javier-Gaytan-Cervantes/publication/334985527_Presence_of_HP_V_DNA_in_extracellular_vesicles_from_HeLa_cells_and_cervical_samples/links/5e1caffb299bf10bc3abd9d9/Presence-of-HPV-DNA-in-extracellular-vesicles-from-HeLa-cells-and-cervical-samples.pdf
 - (46) Landry, Jonathan J M; Theodor Pyl, Paul; Rausch, Tobias; Zichner, Thomas; Tekkedil, Manu M.; Stütz, Adrian M.; Jauch, Anna; Aiyar, Raeka S.; Pau, Gregoire; Delhomme, Nicolas; Gagneur, Julien; Korbel, Jan O.; Huber, Wolfgang; Steinmetz, Lars M. “The Genomic and Transcriptomic Landscape of a HeLa Cell Line.” *G3 Genes|Genomes|Genetics*, Volume 3, Issue 8, 1 August 2013, Pages 1213–1224,
<https://academic.oup.com/g3journal/article/3/8/1213/6025754?versioned=true>
 - (47) Forment, Josep V.; Abderrahmane, Kaidi; Jackson, Stephen P. “Chromothripsis and Cancer: Causes and Consequences of Chromosome Shattering.” *Nature Reviews Cancer*, Volume 12, pages 663-670. <https://www.nature.com/articles/nrc3352>
 - (48) “HeLa.” The Broad Institute.
https://depmap.org/portal/cell_line/HELA_CERVIX?tab=mutation
 - (49) “UBE3A Gene: Ubiquitin Protein Ligase E3A.” National Library of Medicine.
<https://medlineplus.gov/genetics/gene/ube3a/#conditions>
 - (50) “UBE3A Ubiquitin Protein Ligase E3A.” National Library of Medicine. Updated 6 September 2022. <https://www.ncbi.nlm.nih.gov/gene/7337>
 - (51) “CRNKL1 Crooked Neck pre-mRNA Splicing Factor.” National Library of Medicine. Updated 6 September 2022. <https://www.ncbi.nlm.nih.gov/gene/51340>
 - (52) “CRNKL1 Gene.” Harmonizome.
<https://maayanlab.cloud/Harmonizome/gene/CRNKL1>

- (53) “URI1 URI1 Prefoldin Like Chaperone.” National Library of Medicine. Updated 6 September 2022. <https://www.ncbi.nlm.nih.gov/gene/8725>
- (54) “NOL7 Nucleolar Protein 7.” National Library of Medicine. Updated 6 September 2022. <https://www.ncbi.nlm.nih.gov/gene/51406>
- (55) “ABCD1 Gene: ATP Binding Cassette Subfamily D Member 1.” National Library of Medicine. <https://medlineplus.gov/genetics/gene/abcd1/>
- (56) “RPN1 Ribophorin.” National Library of Medicine. Updated 6 September 2022. <https://www.ncbi.nlm.nih.gov/gene/6184>
- (57) “ZER1 zyg-11 Related Cell Cycle Regulator.” National Library of Medicine. Updated 6 September 2022. <https://www.ncbi.nlm.nih.gov/gene/10444>
- (58) “GNHR1 Gonadotropin-Releasing Hormone 1.” National Library of Medicine. Updated 6 September 2022. <https://www.ncbi.nlm.nih.gov/gene/2796>
- (59) Grundker, Carsten; Emons, Gunter. “The Role of Gonadotropin-Releasing Hormone in Cancer Cell Proliferation and Metastasis.” *Front Endocrinology*, Volume 8, Issue 187. <https://www.ncbi.nlm.nih.gov/pmc/articles/PMC5543040/>
- (60) “DCTN1 Gene: Dynactin Subunit 1.” National Library of Medicine. <https://medlineplus.gov/genetics/gene/dctn1/>
- (61) “TNS2 Tensin 2.” National Library of Medicine. Updated 6 September 2022. <https://www.ncbi.nlm.nih.gov/gene/23371>
- (62) “Breast Cancer Types: What Your Type Means.” The Mayo Clinic. <https://www.mayoclinic.org/diseases-conditions/breast-cancer/in-depth/breast-cancer/art-20045654#:~:text=Ductal%20carcinoma%20is%20the%20most,it%27s%20made%2C%20to%20the%20nipple>
- (63) Kleen, Judith; Davidson, Nancy. “The Biology of Breast Carcinoma.” *Skeletal Complications of Malignancy: Cancer Supplement*, 1 February 2003, Volume 97, Number 3. <https://acsjournals.onlinelibrary.wiley.com/doi/pdfdirect/10.1002/cncr.11126>
- (64) “ESR1 Estrogen Receptor 1.” National Library of Medicine. <https://www.ncbi.nlm.nih.gov/gene/2099>
- (65) Guo, Yan Jun; Pan, Wei-Wei; Liu, Sheng-Bing; Shen, Zhong-Fie; Xu, Ying; Hu, Ling Ling. “ERK/MAPK Signaling Pathway and Tumorigenesis (Review).” *Experimental and Therapeutic Medicine*, pages 1997-2007. <https://www.spandidos-publications.com/10.3892/etm.2020.8454>
- (66) “PGR Progesterone Receptor.” National Library of Medicine.” <https://www.ncbi.nlm.nih.gov/gene/5241>
- (67) Scarpin, Katherine; Graham, J Dinny; Mote, Patricia; Clarke, Christine. “Progesterone Action in Human Tissues: Regulation by Progesterone Receptor (PR) Isoform Expression, Nuclear Positioning and Coregulator Expression.” *Nuclear Receptor Signaling*, Volume 7, 2009. <https://www.ncbi.nlm.nih.gov/pmc/articles/PMC2807635/#:~:text=Progesterone%20is%20an%20essential%20regulator,role%20of%20this%20hormone%20in>
- (68) Gutierrez, Carolina; Schiff, Rachel. “HER2: Biology, Detection, and Clinical Implications.” *Archives of Pathology and Laboratory Medicine*, Volume 135, Issue 1, Pages 55-62. <https://www.ncbi.nlm.nih.gov/pmc/articles/PMC3242418/>
- (69) “p53 gene.” National Cancer Institute. <https://www.cancer.gov/publications/dictionaries/cancer-terms/def/p53-gene>

- (70) “Cell Line Profile: MDA-MB-231.” *European Collection of Authenticated Cell Cultures*, Culture Collections, UK Health Security Agency.
<https://www.culturecollections.org.uk/media/133182/mda-mb-231-cell-line-profile.pdf>
- (71) Hui, L; Zheng, Y; Yan, Y; Bargonette, J; Foster, DA. Mutant p53 in MDA-MB-231 Breast Cancer Cells is Stabilized by Elevated Phospholipase D Activity and Contributes to Survival Signals Generated by Phospholipase D.” *Onconge*, Volume 25, 2006, pages 7305-7310.
https://www.researchgate.net/profile/Jill-Bargonetti/publication/6998048_Mutant_p53_in_MDA-MB-231_breast_cancer_cells_is_stabilized_by_elevated_phospholipase_D_activity_and_contributes_to_survival_signals_generated_by_phospholipase_D/links/57acbaa308ae42ba52b25d69/Mutant-p53-in-MDA-MB-231-breast-cancer-cells-is-stabilized-by-elevated-phospholipase-D-activity-and-contributes-to-survival-signals-generated-by-phospholipase-D.pdf
- (72) MacMahon, Brian. “Epidemiology and the Causes of Breast Cancer.” *International Journal of Cancer*, Volume 118, pages 2373-2738.
<https://onlinelibrary.wiley.com/doi/pdf/10.1002/ijc.21404>
- (73) Key, Timothy; Verkasalo, Pia; Banks, Emily. “Epidemiology of Breast Cancer.” *The Lancet Oncology*, Volume 2, Issue 3, pages 133-140.
https://www.sciencedirect.com/science/article/pii/S1470204500002540?casa_token=IuO2BbAPriMAAAAAA:z7-sN8ITAVGsLLQLxUQv7h4ZHCJgv1hM8IPCNeOWX6apuOOmiqvGi2CMU5RnpMxLYZ6x1wD5wak
- (74) “MDAMB231.” The Broad Institute.
https://depmap.org/portal/cell_line/HELA_CERVIX?tab=mutation
- (75) Audrito, Valentina; Messana, Vincenzo; Delagio, Sivlia. “NAMPT and NARPT: Two Metabolic Enzymes with Key Roles in Inflammation.” *Frontiers in Oncology*, 19 March 2020. <https://www.frontiersin.org/articles/10.3389/fonc.2020.00358/full>
- (76) “WDR73 WD Repeat Domain 73.” National Library of Medicine.
<https://www.ncbi.nlm.nih.gov/gene/84942>
- (77) “SNRPB2 Small Nuclear Ribonucleoprotein Polypeptide B2.” National Library of Medicine.
<https://www.ncbi.nlm.nih.gov/gene?Db=gene&Cmd=DetailsSearch&Term=6629>
- (78) “UBIAD1 UbiA Prenyltransferase Domain Containing 1.” National Library of Medicine. <https://www.ncbi.nlm.nih.gov/gene/29914>
- (79) “PELO Pelota mRNA Surveillance and Ribosome Rescue Factor” National Library of Medicine. <https://www.ncbi.nlm.nih.gov/gene/53918>
- (80) “BRAT1 BRCA1 Associated ATM Activator 1.” National Library of Medicine.
<https://www.ncbi.nlm.nih.gov/gene/221927>
- (81) “ADSS2 Adenylosuccinate Synthase 2.” National Library of Medicine.
<https://www.ncbi.nlm.nih.gov/gene/159>
- (82) “Adenosine Mohophosphate.”
<https://wa.kaiserpermanente.org/kbase/topic.jhtml?docId=hn-2796008>
- (83) “SLC4A7 Solute Carrier Family 4 Member 7.” National Library of Medicine.
<https://www.ncbi.nlm.nih.gov/gene/9497>
- (84) “RAB7A RAB7A, Member RAS Oncogene Family.” National Library of Medicine.
<https://www.ncbi.nlm.nih.gov/gene/7879>

- (85) "ELMO2 Engulfment and Cell Motility 2." National Library of Medicine. <https://www.ncbi.nlm.nih.gov/gene/63916>
- (86) Kumar, Anuj; Pathak, P; Dass, N. "A Study of Speed of Sound in Water." *Journal of Applied Physics*, Volume 8, Issue 4, pages 21-23. https://www.researchgate.net/profile/Pp-Pathak/publication/306341925_A_Study_of_Speed_of_Sound_in_Water/links/57c5511b08ae76231545ef5a/A-Study-of-Speed-of-Sound-in-Water.pdf
- (87) Bamber, JC; Hill, CR. "Ultrasonic Attenuation and Propagation Speed in Mammalian Tissues as a Function of Temperature." *Ultrasound in Medicine & Biology*, Volume 5, Issue 2, pages 149-157. <https://www.sciencedirect.com/science/article/abs/pii/0301562979900838>
- (88) Geiger, Thomas; Peeper, Daniel. "Metastasis Mechanism." *Biochimica et Biophysica Acta - Reviews on Cancer*, Volume 1796, Issue 2, pages 293-308. <https://www.sciencedirect.com/science/article/pii/S0304419X09000535>
- (89) Fischer, Edgar. "Nuclear Morphology and the Biology of Cancer Cells." *Acta Cytological*, Volume 64, pages 511-519. <https://www.karger.com/Article/PDF/508780>